IMPACT OF BREECH GEOMETRY AND PROPELLANT FLOW ON THE RELEASE OF LARGE PELLETS FOR THE ITER DISRUPTION MITIGATION SYSTEM

T. E. GEBHART[1], L. R. BAYLOR[1], M. DIBON[4], M. N. ERICSON[1], E. J. FELSKE[2], S. S. FRANK[1], W. L. GARDNER[1], A. G. GHIOZZI[3], S. JACHMICH[4], U. KRUEZI[4], M. LEHNEN[4], AND D. A. VELEZ[5]
[1]Oak Ridge National Laboratory, Oak Ridge, TN, USA
[2]Columbia University, New York City, NY, USA
[3]Oak Ridge Associated Universities at General Atomics, San Diego, CA, USA
[4]ITER Organization, Saint Paul Les Durance, France
[5]University of Wisconsin-Madison, Madison, WI, USA
E-mail: GebhartGE@ornl.gov

Abstract

Studies have been performed on the release mechanism for large pellets using high pressure gas in a shattered pellet injector. Typically, pellets are dislodged from the cryogenic surface and accelerated down a barrel using high pressure gas delivered by a fast-acting propellant valve. The pellets impact an angled surface which shatters the pellet into many small fragments before entering the plasma [1]. This technique was initially demonstrated on DIII-D [2] and is now deployed on JET [3, 4], KSTAR [3], ASDEX-Upgrade, and other tokamaks around the world in support of ITER's disruption mitigation system design and physics basis. The large hydrogen, 28.5 mm diameter, 2 length-to-diameter ratio, pellets foreseen for ITER SPI operation have low material strength and low heat of sublimation, which cause the pellets to be fragile and highly reactive to the impact of warm propellant gas. Due to the size of the pellets, significantly more propellant gas is required to dislodge and accelerate them. This creates a potentially significant propellant gas removal issue as 2 to 6 bar-L of gas is expected to be required for release and speed control. The research presented in this paper is an in-depth exploration of the parameters that are keys to reliable pellet release and speed control. Computational fluid dynamics (CFD) modeling of propellant flows through various breech designs was conducted to determine the force generated on the back surface of a pellet. These simulations assumed the use of the ORNL designed flyer plate valve [5,6]. CFD modeling combined with experimental measurements provide adequate insight to determine a path to an optimal valve and breech design for ITER SPI pellet release and speed control while minimizing propellant gas usage.

1. BACKGROUND AND INTRODUCTION

Disruption mitigation (DM) using shattered pellet injection (SPI) on ITER must be a reliable and predictable system to ensure it is effective at successfully mitigating the possible deleterious effects that result from a disruption. Reducing heat loads, reducing electromagnetic loads, and preventing the formation of runaway electron beams or disbursing runaway electron beams that do form are the primary purpose of the DM system. Without proven reliability, ITER risks significant damage to the plasma facing components and supporting structure. Shattered pellet injection is a process that utilizes cryogenics to desublimate material onto the inner surface of a pipe gun barrel. Pellets are typically comprised of D_2 or H_2 mixed with a small amount (~10% by mole) of high-Z material, typically neon. ITER SPI pellets will be 28.5 mm in diameter and have a length-to-diameter (L/D) ratio of 2. Pellets are dislodged and accelerated down a barrel by a pulse of high pressure (~60 bar) gas delivered by a fast-opening propellant valve. Pellets are fired down stream into an angled tube or plate, causing them to break into many small fragments before entering the plasma. Shattered pellet injection has been studied and explored on tokamaks around the world to inform the ITER DM design and physics baseline [2-4, 7-8]. The fragmentation process was first explored in a laboratory setting to determine the parameters that affect pellet shattering [1]. The newly understood fragmentation process led to various fragmentation properties being explored on ASDEX-U [7] and JET. The modifications made to the JET SPI [8] system to allow for slower speeds, along with laboratory testing of ITER sized SPI pellets [9-11] led to the realization that pellet release with minimal propellant gas usage becomes increasingly important for the reliability of DM with large H_2 pellets on ITER.

The ITER DM system consists of 27 independent SPI guns, 24 of which are located in three equitorial ports in drawers containing six guns each. The other three guns are located in three separate upper ports. Figure 1 shows multiple pictures of the ITER SPI system, from an upper level of the location on the machine [12], to one individual flight path. The individual flight path is labeled with some of the various challenges that are to be addressed through planned R&D.

Optimization of the pellet launching portion of the ITER SPI system is essential to ensure reliable release and acceleration of pellets and their intact delivery to the plasma. Optimizing the design of the propellant valve, breech geometry, barrel, and downstream gas removal volumes are all essential for meeting the requirements of the ITER SPI system. Those requirements are; to ensure a high reliability of intact pellet delivery with reliable control of H_2 pellet speeds from 300 to 500 m/s, to minimize the heat load on the pellet formation coldhead from the breech-

barrel system, to use as little propellant gas as possible to launch pellets and retain that propellant gas to prevent it from entering the plasma prior to the pellet, and to meet explosive gas inventory limits in the port cells. The research outlined in this paper will address valve operation, pellet release, dispersion reduction, and propellant gas reduction using experimental data and observations, along with CFD modeling to determine a methodology for optimizing the valve-breech system design.

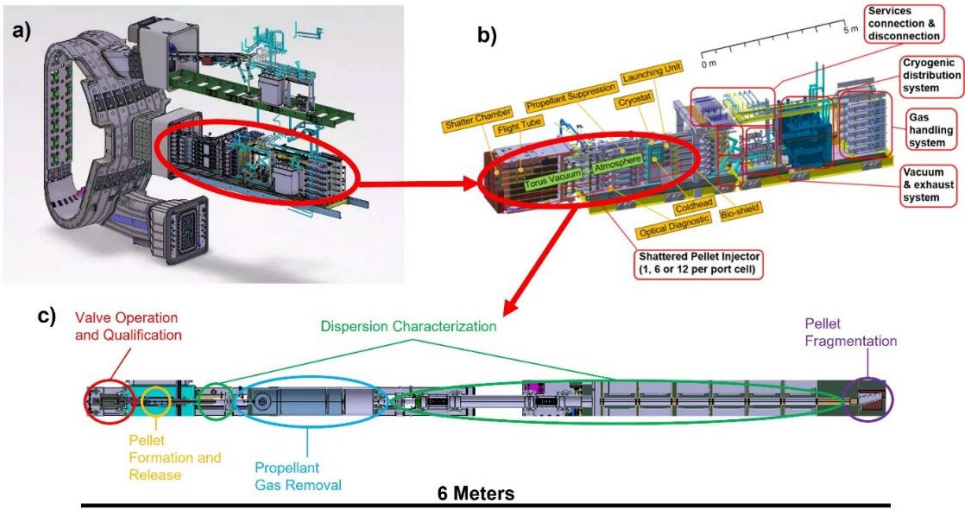

Fig. 1. a) A view of one section of ITER where 13 of the SPIs are located, 12 equitorially, and one in the upper port [Image Courtesy of the ITER Organization]. b) an image of the port containing 12 SPIs with labels showing the subsystems [13]. c) a single SPI flight path with labels showing some of the open R&D needed for the ITER SPI system.

2. PELLET RELEASE ANALYSIS USING EXISTING EQUIPMENT

Previous experimental results have been compiled and used to compare with CFD modeling of forces generated on pellets by gas delivered from various valves. Two types of propellant valves were used in this study, a large flyer plate valve (FPV) [5] and a solenoid operated valve [14]. The large FPV has an outlet diameter of 24.5 mm, has a plenum volume of 0.75 L, and operates at maximum 60 bar plenum pressure. It utilizes a capacitive discharge from a prototype high voltage (HV) (~3 kV) power supply [15] to drive a current through a pancake coil that is closely coupled to an aluminum disk called the 'flyer plate'. The change in magnetic field, dB/dt, induces eddy currents in the flyer plate which repel the field and generate a force large enough to open the valve. The FPV is designed to operate in a background magnetic field, although a significant torque is generated due to the eddy current interaction with the background field [5], and it has yet to pass required lifecycle testing. A typical shot opens the valve ~2-4 mm and delivers from 2 – 6 bar-L of H_2 propellant. The residual pressure in the plenum re-seats the valve after firing. The solenoid valve operates using a custom power supply with a maximum voltage of ~180 V. This type of valve has been deployed for SPI, pellet fueling, and edge localized mode pacing experiments worldwide. It has a 6 mm opening, has a variable plenum volume, and can operate between 40 and 70 bar. For the experiments discussed in this paper, the plenum volume of the solenoid valve was 0.315 L. Figure 2 below shows CAD images of the two valves.

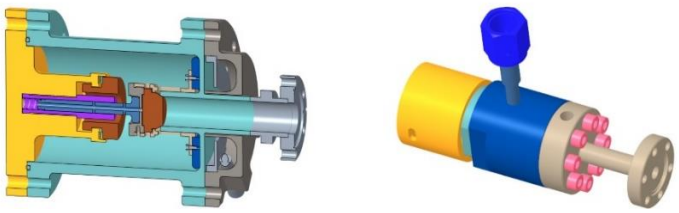

Fig. 2. CAD images of the propellant valves used to fire large H_2 pellets. The large FPV (left) has an opening of 24.5 mm with a volume of ~0.75 L and the solenoid valve (right) has an opening of 6 mm with a 0.315 L volume for the experiments discussed in this paper.

Flow rates from these valves were calculated using the measured pressure drop in the valve plenums. The pressure sensors used to make the measurements for these calculations have a temporal resolution of <1 µs. The flow rates from two FPV shots and one solenoid valve shot are shown in Fig. 3. The two FPV shots delivered 2.5 and 5.6 bar-L of H_2 propellant and were fired using capacitor charges of 1.2 and 1.35 kV. The solenoid valve shot had a set pulse width of 1.9 ms and delivered 2.2 bar-L of H_2 propellant. Images of H_2 pellets fired by these shots

are shown in Fig. 3. The large FPV typically results in broken H_2 pellets due to the large impulse of gas delivered to the rear surface of the pellet. This impulse was quantified using STAR CCM+ [16], where CFD modeling was conducted to quantify the force on the rear of the pellet [17] from the 2.5 bar-L large FPV shot and the solenoid valve shot shown in Fig 3. Figure 4 shows two plots. The plot on the left shows the total integral force applied to the rear of the pellet from the resultant momentum and pressure rise of the impacting gas. The plot on the right shows the minimum and maximum forces calculated on the mesh cells that mimic the pellet face during each of these shots. The difference in the maximum integral force bewteen the two shots is due to the reduction in breech volume when the solenoid valve is installed. The breech volume on the ITER SPI test bed [9] at Oak Ridge National Laboratory (ORNL) is ~0.11 L with the large FPV installed and 0.054 L with the solenoid valve installed. The FPV shot exhibits a large spike in differential pressure, as shown by the plot on the right in Fig 4. The majority of this force is applied to the center of the pellet over the short duration of force disparity. The lower flow rate from the solenoid valve results in a low-impulse and gradual increase of force with very little force differential over the face of the pellet. This CFD modeling does not account for the pellet dislodging and accelerating down the barrel. The plot on the right in Fig. 4 also labels the measured breakaway pressure of a pure 28.5 mm, 2 L/D H_2 pellet.

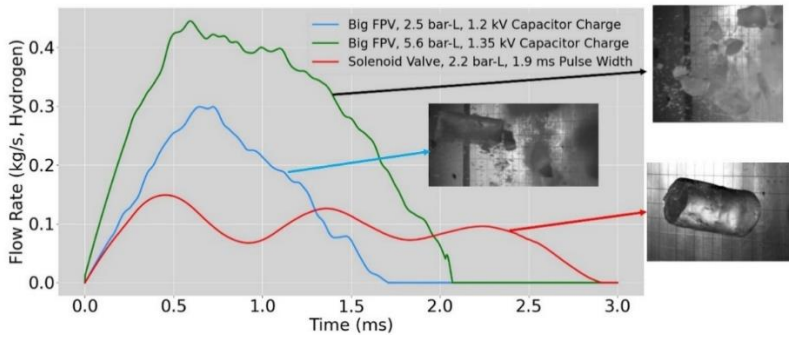

Fig. 3. Flow rates calculated from the plenum pressure drop for two typical large FPV shots and one typical solenoid valve shot. Images of the resulting pellets are shown for each shot.

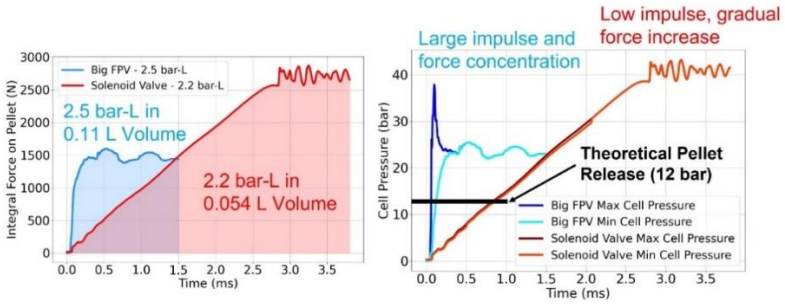

Fig. 4. (Left) The total integral force applied to the pellet from the 2.5 bar-L large FPV shot and the solenoid valve shot shown in Fig. 3. (Right) The minimum and maximum forces calculated over mesh cell areas on the pellet face for each of the two shots shown in the plot on the left.

3. EFFECT OF BREECH MODIFICATIONS ON PELLET RELEASE

It was hypothesized that inserting breech geometry modifiers could be used to tailor the flow to the rear of the pellet and overall pressure rise in the breech to optimize pellet release. Two geometries were explored, a conical breech volume reducer and a nozzle-shaped breech volume reducer. On the SPI testbed at ORNL, the breech volume with the large FPV installed is ~0.11 L. Both of these reducers decrease the volume by 0.03 L. Figure 5 shows CAD images of the breech modifiers installed on the ITER SPI testbed at ORNL. These geometries were used in STAR CCM+ to conduct similar CFD modeling as described in the previous section of this paper. The 2.5 bar-L large FPV shot shown in Fig. 3 was used as a flow rate input for the modified breech scenarios. The solenoid valve was not explored for use with the breech modifiers. Figure 6 shows the results of the CFD using the modified breech geometries. The plot on the left in Fig. 6 shows the total integral force imparted to the rear of the pellet from the propellant gas pulse. The total impulse seen by the pellet is greater with the conical reducer, as the nozzle reducer decreases the overall flow to the pellet. The nozzle reducer does, however, impart a large differential force across the pellet face during the initial 0.1 ms of gas flow. Experiments were conducted with these breech modifiers to explore the impact they have on pellet release. The large FPV was used to fire 28.5 mm H_2 pellets. Typical results are shown in Fig. 7 below. Although the nozzle reducer imparts a large differential force, it increased the reliability of firing intact pellets due to the smaller overall impulse. Roughly 50% of pellets fired using the nozzle reducer were intact, a significant increase from the non-modified breech case. The conical

reducer imparts a significant impulse on the pellet face and resulted in 0 intact H_2 pellets during these experiments. The exploration of these breech modifiers resulted in a better understanding of H_2 pellet survivability, such as the ability of these pellets to withstand a large force disparity from the center of the pellet to the edge as long as the overall impulse remains relatively low.

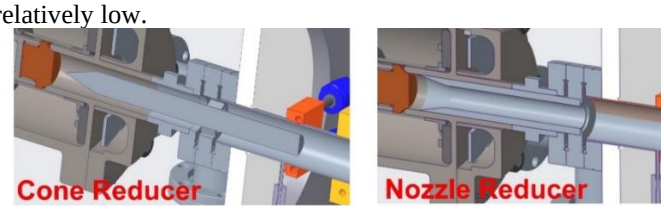

Fig. 5. Labeled CAD images of the two breech modifiers, the cone reducer (left) and the nozzle reducer (right) explored in this paper.

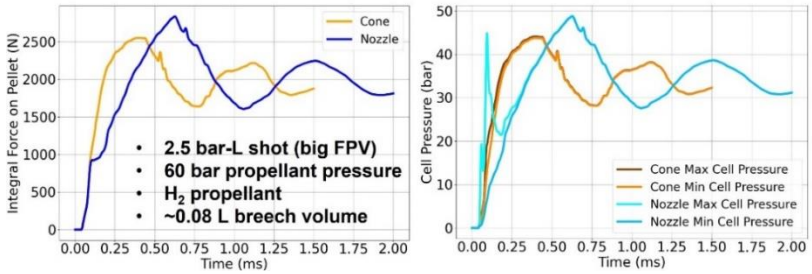

Fig. 6. (Left) The total integrated force on the rear of the pellet from the impinging propellant gas from a 2.5 bar-L large FPV shot as calculated using CFD for the two modified breech geometries. (Right) The minimum and maximum mesh cell pressures calculated for each of the two shots shown in the plot on the left.

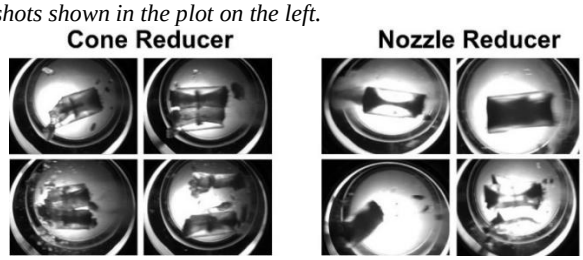

Fig. 7. Images of pellets fired by the large FPV with the cone reducer and nozzle reducer breech modifiers installed.

4. NEW VALVE DESIGN AND MODELING

The previous sections of this paper discussed the large impulse incident on the rear face of the pellet when propellant is delivered by the large FPV due to the large 24.5 mm opening of the valve. The 0.75 L plenum volume of the large FPV also resulted in exceeding the explosive gas limits in the port cell. At 60 bar, each large FPV contains 45 bar-L of H_2, three times the amount that is needed per valve to meet specifications. The solenoid valve is not capable of working in a background magnetic field without magnetic shielding. The small, 6 mm, opening of the solenoid valve provided an adequate flow rate to release and accelerate H_2 pellets to the required 500 m/s speed. Comparing these two results led to the decision that a smaller FPV should be designed. A series of modeling efforts were undertaken to better understand the impact of the valve and breech design on the forces imparted on the pellets by the propellant gas, and the resulting downstream pellet speeds. The small FPV design has a volume of 0.25 L with an opening of 8 mm. It is driven by the same HV pulsed power supply that drives the original large FPV. Figure 8 shows a CAD image of the newly designed FPV.

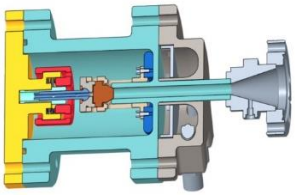

Fig. 8. A CAD model image of the small FPV with a plenum volume of 0.25 L and an outlet diameter of 8 mm.

Using measured characteristics of the existing pulsed power supply, along with calculated theoretical values for the small FPV coil resistance and inductance, a series of simulations were conducted to model the discharge current through the valve coil for a range of initial capacitor charges (from 800 to 1000 V). These simulations were conducted in LTSpice [18]. Figure 9 shows a plot of these simulated currents for the small FPV coil. The characteristics of the large FPV coil were used in this model and the results were compared to the measured

current. The simulated current varied from the measured current by less than 4% at any given time throughout the discharge.

To determine the resulting electromagnetic dynamics of the valve internals, the simulated currents were used as an input to an ANSYS Maxwell [19] model of the small valve. The ANSYS model was used to determine the electromagnetic forces on the valve internals. The force required to open the valve is the product of the opening area times the pressure in the plenum (60 bar). This model does not account for pressure drop within the plenum, introducing some error in the resulting closing force. The energy required to accelerate the valve internals after the opening force has been overcome is proportional to the inertial mass of the moving parts within the valve. The equation of motion used in this model only accounts for motion along the axis of the valve. The resulting valve displacement curves are shown in Figure 10, labeled by the initial capacitor voltage. Due to the larger dB/dt and the magnetic inertia within the valve, the higher current shots hold the valve open longer. This effect has been seen during testing of the large FPV as well.

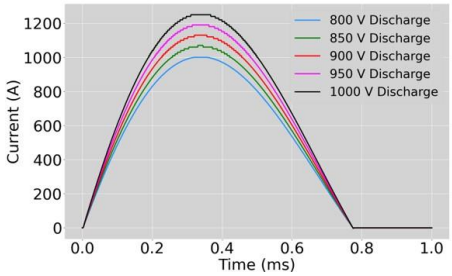

Fig. 9. Current traces simulated using measured values from the existing pulsed power supply and the calculated resistance and inductance for the small FPV pancake coil. Traces are labeled with the initial capacitor charges for each shot.

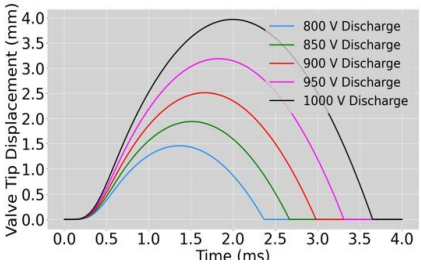

Fig. 10. The valve tip displacement for each current trace shown in Fig. 9 as calculated by ANSYS Maxwell.

Using the calculated tip displacements, CFD was conducted in STAR CCM+ to model the flow out of the valve using the ORNL ITER SPI test bed valve and breech geometry. The downstream outlet boundary condition was set as a pressure outlet, allowing gas to flow freely from the valve out of the barrel. The length of the breech, beyond the opening of the valve does not limit the flow, as the main limiting conductance is the 8 mm valve exit. Figure 11 shows the resulting flow rates for each of the five shots modeled, labeled by the initial capacitor voltage. Comparing the flow rates in Fig. 11 to the flow rates from the large FPV and the solenoid valve, the small FPV has the capability to deliver gas in a more controlled way than the large FPV and can deliver more gas than the solenoid valve due to the larger conductance of the valve outlet. The rise time of the flow rates are significantly slower than the rise time of the large FPV and comparable to the solenoid valve, which was sucessful in firing large H_2 pellets.

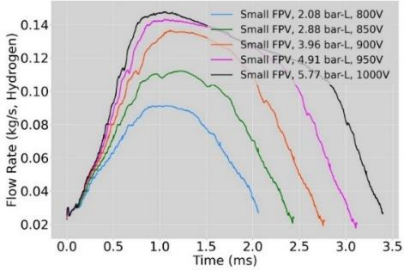

Fig. 11. Propellant flow rates from the small FPV design as calculated in STAR CCM+ including a moving valve tip dictated by the displacement curves shown in Fig. 10. The plenum was initially filled with 60 bar hydrogen for these simulations.

Similar to the data discussed in previous sections, CFD modeling was conducted with STAR CCM+ using the valve flow rates shown in Fig. 11 for the 800, 900, and 1000 V cases as inputs to determine the total force and the minimum and maximum mesh cell forces on the rear face of the pellet. These simulations do not account for the pellet releasing and moving down the barrel and are intended to explore the initial impulse on the pellet before it is displodged to compare to the large FPV and solenoid valve shots. The results from these CFD simulations

are shown in Fig. 12. The 800 V shot delivers the same 2.08 bar-L of propellant gas as shown in Fig. 11. The 900 and 1000 V shots deliver less gas than shown in Fig. 11 due to the wall boundary condition (pellet surrogate) affecting the flow rate from the valve as gas hits the pellet and propagates back into the valve plenum. Realistically, this is unlikeley to happen with pure H_2 pellets as they will release on a faster time scale. The gas delivered beyond the point of pellet release is utilized for pellet acceleration as it helps maintain the accelerating pressure behind the pellet.

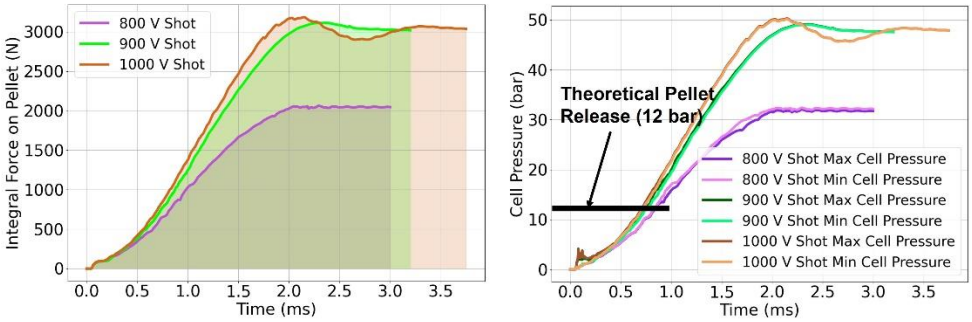

Fig. 12. (Left) The total integrated force on the rear of the pellet from the impinging propellant gas from the 800, 900 and 1000 V small FPV shots as calculated using CFD of the current breech geometry of the ORNL ITER SPI test bed . (Right) The minimum and maximum mesh cell pressures calculated for each of the shots shown in the plot on the left.

5. BREECH OPTIMIZATION AND FORCES ON PELLET

A code was written in Python to calculate the dynamic processes of the pressure rise behind the pellet, the pellet breaking away, and the subsequent acceleration of the pellet down the barrel. Figure 13 shows a basic diagram of the geometry and parameters used to model these effects. The code requires a flow rate input to build pressure to release and accelerate the pellet. The driving force behind the pellet is a simple pressure rise calculated by the inflow of propellant. Previous models [20] for these systems have accounted for shock mechanics and rarefraction propagation in the breech. When including these phenomenon in the Python code, it was found that they resulted in an overestimate of pellet speed by ~25% when compared to experimental SPI results using the solenoid valve. The combination of low flow rates and large breech volumes result in very little shock formation as observed in the CFD modeling used to calculate the force on the rear of the pellet. Validation of the Python code was done by comparing the resulting experimental speed from the solenoid valve pulse, shown in Fig. 3, to the speed calculated by the model. The experimentally measured pellet speed from this shot was 445 m/s and the code predicted a speed of 451 m/s. The code requires the user to input a required breakaway pressure so that pellet acceleration can be initiated.

The calculated flow rates for the 800, 900, and 1000 V shots shown in Fig. 11 were used as inputs for this analysis, where various initial breech volumes were scanned. Other constant inputs that were used are a 12 bar pellet release pressure, a 3.2 g pellet mass, an 830 mm barrel length (current ITER design), and a minimum volume of 0.014 L, which is the fixed volume of the valve outlet. The additional breech volume is calculated using a fixed diameter of 28.5 mm. Breech volumes are varied by changing the length of the breech.

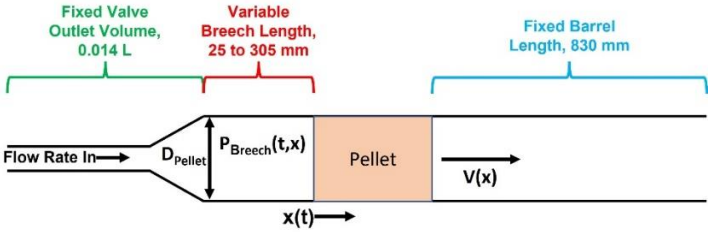

Fig. 13. A diagram of the parameters used in the breech optimization code to determine the effects of varying the breech length on resulting pellet speed and pressure behind the pellet as it leaves the barrel.

Figure 14 below shows a series of plots that outline the temporal evolution of breech pressure and pellet speed as calculated by the Python code using the flow rates from the 800, 900, and 1000 V shots as an input. The multiple curves show a scan over various breech volumes and, as described previously, breech volumes are varied by only changing the length of the 28.5 mm segment of barrel between the pellet and valve connection. Table 1 shows the resulting pellet speeds and final pressures behind the pellet as it exits the barrel. The general trends shown in these modeling results suggest that a larger breech volume is ideal for limiting the final pressure in the barrel (ideal for dispersion reduction) and that as the breech volume decreases, pellet speed will increase until the breech volume gets too small and the pellet leaves the barrel prior to the valve closing, resulting in delivery of

excess propellant gas. The cases for the 1000 V shots result in pellet speeds that exceed the requirement of 500 m/s. Since the 1000 V shot delivers more gas over the 3.5 ms delivery time than the other shots, the breech pressures remain higher. The four smaller breech volumes result in the pellet leaving the barrel before the valve is finished delivering gas, making this scenario not ideal. The 800 V shot resulted in falling short of the 500 m/s pellet speed requirement by a small margin. For this shot, the required breakaway pressure of 12 bar [21] is not met by the 2.08 bar-L of propellant delivered in the two larger breech volumes. The 900 V shot resulted in exceeding the 500 m/s pellet speed requirement for all cases but the largest breech. The pellets also do not leave the barrel until the valve completes delivery of propellant gas. Out of these three cases, this scenario is the best case. Other cases will be explored outside of this paper with the goal of reducing the amount of propellant gas required and optimizing the breech volume with the release timing and propellant flow duration.

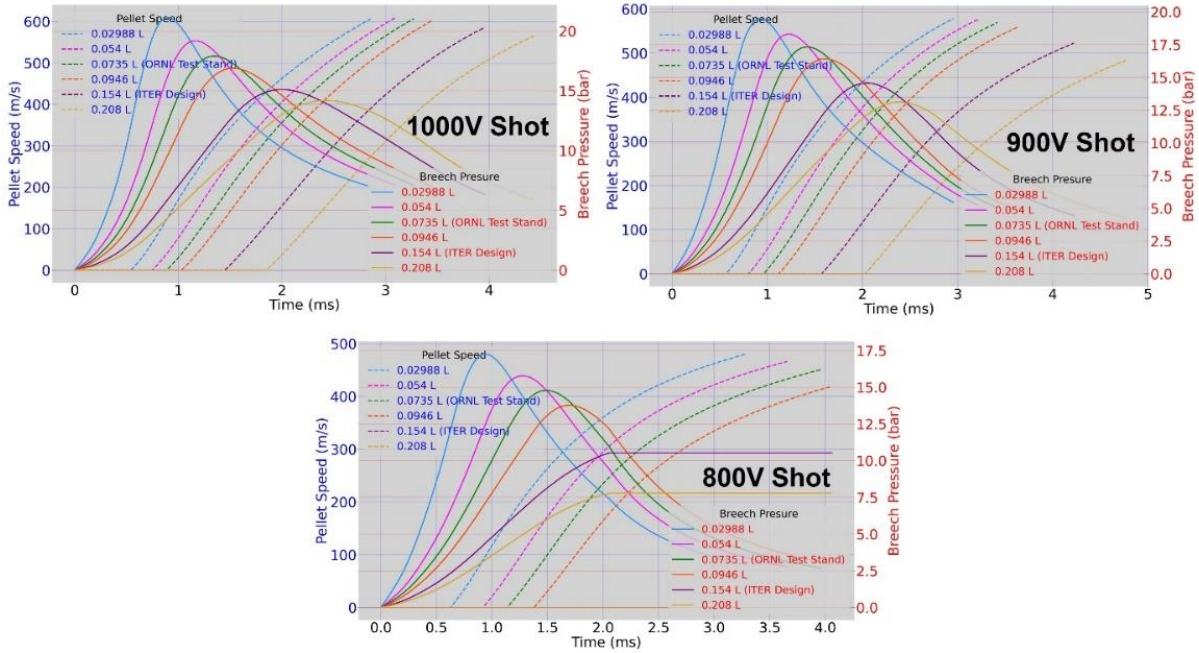

Fig. 14. Pellet speed and breech pressure curves for 800, 900, and 1000 V small FPV shots over a range of initial breech volumes. These plots display the dynamic effects of the various pulses on the resulting pellet speeds and pressures behind the pellet as they exit the barrel. The barrel length used for these calculations was 830 mm, which is taken from the current ITER SPI design.

Table 1. Resulting speeds of 28.5 mm H_2 pellets and pressures behind the pellets as they leave the 830 mm long barrel for the 800, 900, and 1000 V shots.

	1000 V – 5.78 bar-L		900 V – 3.96 bar-L		800 V – 2.08 bar-L	
Breech Volume (L)	Final Pellet Speed (m/s)	Final Pressure (Bar)	Final Pellet Speed (m/s)	Final Pressure (Bar)	Final Pellet Speed (m/s)	Final Pressure (Bar)
0.0298	606.1	6.99	578.7	5.45	480.5	2.9
0.054	609.4	7.13	576.9	5.23	466.5	2.77
0.0735	607.2	7.1	569.2	5.06	451.3	2.69
0.945	603.3	6.95	558.2	4.89	419.2	2.94
0.154	586.4	6.3	522.9	4.47	No Release	No Release
0.208	565.6	5.9	483.7	4.27	No Release	No Release

6. DISCUSSION AND FUTURE RESEARCH

Through experiments and modeling it was determined that tailoring propellant flow rate and optimizing the breech volume for the ITER SPI system is essential for overall reliability and efficient pellet speed control for the ITER SPI system. The use of large diameter (28.5 mm) H_2 pellets requires careful control of the forces imparted to the pellets during the release process. Previous SPI designs never had to account for these issues due the the small pellet sizes (typically <12.5 mm) and the use of D_2 as a base pellet material. Small diameters reduce conductance of propellant to the pellets, limiting impulse, and D_2 is about twice as strong as H_2, making it more robust to impulse forces. Experiments using the large FPV yielded broken H_2 pellets due to the large impulse imparted on the pellets from the relatively large flow rate out of the 24.5 mm valve opening. Other experiments

were conducted using a small diameter (6 mm opening) solenoid operated valve. These experiments yielded sucessfully released, intact, H_2 pellets. CFD modeling was utilized to determine the differences in forces applied to pellets from the gas delivered by these valves. Modeling showed that the impulse from the large FPV is significant and is likely the cause of broken pellets.

A smaller FPV was designed to deliver flow rates tailored to reliably fire large H_2 pellets and to reach the required 500 m/s pellet speed. The small FPV will be operated by the same, existing, pulsed power supply that operates the present large FPV. Using measured parameters from the components of this power supply and the estimated resistance and inductance of the small FPV coil, simulations were conducted in LTSpice to determine the resulting coil currents for a range of initial capacitor charges. These currents were used as an input to an ANSYS Maxwell model of the small FPV to simulate the electromechanical operation of the valve and to determine tip displacement curves. The tip displacement curves were used as an input to STAR CCM+ for CFD modeling. Two CFD models were used; 1) to determine the outlet flow rates from the valve using a pressure outlet where the pellet would be, and 2) to determine the force applied to the pellets using the geometry of the ORNL ITER SPI test bed using a wall boundary condition where the pellet would be located. The outlet flow rates were used in a dynamic systems model to study the trends associated with varying initial breech length and inlet flow rates on the resulting pellet speeds and barrel pressures. The results reported in this paper are intended to inform the design of the ITER SPI system to increase the reliability of intact pellet delivery and pellet speed control.

ACKNOWLEDGEMENTS

This manuscript has been authored by UT-Battelle, LLC under Contract No. DE-AC05-00OR22725 with the U.S. Department of Energy. The United States Government retains and the publisher, by accepting the article for publication, acknowledges that the United States Government retains a non-exclusive, paid-up, irrevocable, world-wide license to publish or reproduce the published form of this manuscript, or allow others to do so, for United States Government purposes. The Department of Energy will provide public access to these results of federally sponsored research in accordance with the DOE Public Access Plan (http://energy.gov/).

The views and opinions expressed herein do not necessarily reflect the views and opinions of the ITER Organization.

REFERENCES

1. GEBHART, T.E., et al., Experimental pellet shatter thresholds and analysis of shatter tube ejecta for disruption mitigation cryogenic pellets, IEEE Transactions on Plasma Science, 48 (6), 1598-1605 (2020).
2. COMMAUX, N., et al., First demonstration of rapid shutdown using neon shattered pellet injection for thermal quench mitigation on DIII-D, Nucl. Fusion, Vol. 56, Mar. 2016, Art. No. 046007.
3. BAYLOR, L.R., et al., Design and performance of shattered pellet injection systems for JET and KSTAR disruption mitigation research in supprt of ITER, Nucl. Fusion, Vol. 61, Aug. 2021, Art. No. 106001.
4. JACHMICH, S., et al., Shattered pellet injection experiments at JET in support of the ITER disruption mitigation system design, Nucl. Fusion, Vol. 62, Dec. 2021, Art. No. 026012.
5. GEBHART, T.E., et al., Design and testing of a prototype eddy current actuated valve for the ITER shattered pellet injection system, IEEE Transactions on Plasma Science, 50 (11), 4177-4181 (2022).
6. LYTTLE, M.S., et al., "Fast acting eddy current driven valve for massive gas injection on ITER", 2015 IEEE 26th Symposium on Fusion Engineering (SOFE), Austin, TX, 2015.
7. DIBON, M., Design of the shattered pellet injection system for ASDEX Upgrade, Rev. Sci. Inst., 94, 043504 (2023)
8. GEBHART, T.E. et al., Modifications to the JET shattered pellet injector to optimize disruption mitigation experiments for supporting ITER's DMS design, IEEE Trans. Plasm. Sci., Submitted for publication
9. GEBHART, T.E., et al., Recent progress in shattered pellet injection technology in support of the ITER disruption mitigation system, Nucl. Fusion, Vol. 61, Sept. 2021, Art. No. 106007.
10. MANZAGOL, J., et al., Simulations and developments for large pellet formation and acceleration for shattered pellet injection of the ITER DMS, Fus. Eng. and Des., Vol. 191, June 2023, 113665.
11. ZOLETNIK, S., et al., Shattered pellet injection technology development in the ITER DMS test laboratory, Fus. Eng. And Des., Vol. 190, May 2023, 113701
12. LEHNEN, M., et al., R&D For Reliable Disruption Mitigation in ITER, IAEA FEC Proceedings, 2018.
13. LUCE, T.C., et al., Progress on the ITER DMS design and integration, IAEA FEC Proceedings 2021.
14. MILORA, S.L., et al., Fast-opening magnetic valve for high-pressure gas injection and applications to hydrogen pellet fueling systems, Rev. Sci. Instrum., Vol. 57, No. 9, pp. 2356-2358, Sept. 1986.
15. ERICSON, M.N., et al., A prototype high-voltage pulsed power supply for control of the ITER shattere pellet injection system flyer plate valve, IEEE Transactions on Plasma Science, 50 (11), 4182-4186 (2022).
16. https://plm.sw.siemens.com/en-US/simcenter/fluids-thermal-simulation/star-ccm/
17. GHIOZZI, A.G., et al., Pressure Response Optimization of an Eddy Current Driven Flyer Plate Valve for the ITER shattered Pellet Injection System, Fusion Sci. and Technol., Vol. 77, Issue 7-8, pp. 915-920, March 2021.
18. https://www.analog.com/en/design-center/design-tools-and-calculators/ltspice-simulator.html
19. https://www.ansys.com/products/electronics/ansys-maxwell
20. J. T. Hogan, et. al., A model for pneumatic pellet injection, Oak Ridge National Laboratory Technical Report, ORNL/TM-8601, July 1983
21. Private communication with F. Millet, CEA Grenoble